A Hygrothermal Risk Analysis Applied to Residential Unvented Attics

Simon Pallin, PhD

Manfred Kehrer
Member ASHRAE

William A. Miller, PhD
Member ASHRAE

ABSTRACT

A residential building, constructed with an unvented attic, is a common roof assembly in the United States. The expected hygrothermal performance and service life of the roof are difficult to estimate due to a number of varying parameters. Typical parameters expected to vary are the climate, direction, and slope of the roof as well as the radiation properties of the surface material. Furthermore, influential parameters are indoor moisture excess, air leakages through the attic floor, and leakages from air-handling unit and ventilation ducts. In addition, the type of building materials such as the insulation material and closed or open cell spray polyurethane foam will influence the future performance of the roof.

A development of a simulation model of the roof assembly will enable a risk and sensitivity analysis, in which the most important varying parameters on the hygrothermal performance can be determined. The model is designed to perform probabilistic simulations using mathematical and hygrothermal calculation tools. The varying input parameters can be chosen from existing measurements, simulations, or standards. An analysis is applied to determine the risk of consequences, such as mold growth, rot, or energy demand of the HVAC unit. Furthermore, the future performance of the roof can be simulated in different climates to facilitate the design of an efficient and reliable roof construction with the most suitable technical solution and to determine the most appropriate building materials for a given climate.

INTRODUCTION

A pitched roof is a very common residential building construction in which the attic space can be either ventilated with exterior air or constructed as unvented. The difference between the two alternatives is mainly the location of the thermal resistance. In a ventilated attic, the greater part of the insulation is located in the ceiling plane. As for the unvented attic, the thermal resistance is instead located inside or directly underneath the roof. Subsequently, the attic space in an unvented attic is embraced by the thermal envelope, thus making it a better environment for an HVAC system compared to a vented attic space. An unvented attic also has less energy loss from the air distribution system in comparison with a ventilated attic (Rudd 2005). The more leaky the ductwork is, the greater the energy losses of the HVAC unit (Russell et al. 2007)—which, in a ventilated attic, become very significant. Air leakages from the indoor environment or the duct system may lead to mold growth on the interior surface of the roof (Hagentoft et al. 2008) or result in ice dam creation (Lstiburek 2006). Consequently, there are advantages with an unvented attic compared with a vented attic, at least in terms of energy efficiency. In concerns of moisture safety, though, the performance of an unvented attic is not that obvious; there are other properties of the roof construction and the indoor and outdoor environment that must be taken into account.

There are usually a large number of wood-based materials in a residential pitched roof construction—rafters, ceiling joists, and roof deck sheathing. Unfortunately, a wood surface is a favorable environment for mold growth, depending on available nutrients, humidity, and temperature (Hukka and Viitanen 1999), and rot. Therefore, it is of great concern to prevent critical levels of relative humidity (RH) inside the

Simon Pallin *is a postdoctoral research associate and* ***Manfred Kehrer*** *and* ***William Miller*** *are senior research engineers in Building Envelope Research at Oak Ridge National Laboratory, Oak Ridge, TN.*

attic, which otherwise offers a potential for moisture build up in the wood materials, especially the roof sheathing (Straube et al. 2010). Naturally, air leakages from the air distribution system, leakages between the indoor and attic spaces, as well as leakages to and from the outside environment will influence the RH in the attic. An unvented attic is constructed to prevent leakages to the outdoor environment; hence leakages from the interior and the air distribution system will dominate the unintended air leakages into the attic space. In addition to these air leakages, the water vapor content of the attic air will depend on the indoor and outdoor water vapor content of the air, the dehumidifying effect from the HVAC system, and the indoor moisture generation.

An unvented attic hosting an HVAC system must be considered as a very complex hygrothermal system. The future performance and expected service life of the roof construction will vary due to a number of influencing parameters, referred to as *variables*. These variables are important to include when analyzing the future conditions of an unvented attic in terms of energy efficiency, moisture safety, and durability. However, each parameter must be expected to vary differently, as should their importance on the attic performance; hence, the most decisive parameters can be identified. A range of influencing parameters is as follows:

- Indoor heat and moisture production
- Hygrothermal material properties
- Natural and forced unintended air leakage
- Features of the HVAC system, i.e., dehumidifying/humidifying effect, airflow rate, etc.
- Geometrical variations of the building components
- Outdoor climate
- Orientation and location of the building and slope of the roof
- Workmanship
- User behavior, i.e., HVAC setpoint temperatures, airing, maintenance, etc.

The purpose of this study is to develop a reliable hygrothermal simulation model of an unvented attic, which in the future should facilitate the design of an efficient and reliable roof construction with the most suitable technical solution, and to determine the most appropriate building materials for a given climate. This study focuses on determining the importance of the most decisive parameters and analyzing their sensitivity on the overall hygrothermal performance of the unvented attic. A risk analysis is executed based on simulations with a number of varying parameters, creating different plausible scenarios of realistic attic and roof constructions. The performance indicators of interest in this study are the risk of rot in the wood-based roof sheathing and the risk of mold on roof rafters and ceiling joists. In addition, the impact from the varying parameters on the energy demand of the air distribution system is investigated.

THE SIMULATION MODEL

The unvented attic was simulated with a numerical model created in MATLAB®, which is a software for mathematical computations (MathWorks 2013). This model was then interacted with WUFI1D, which is a validated hygrothermal calculation tool (Künzel 1995). The numerical MATLAB model is designed to calculate the heat and water vapor transfer through the building components and intermediate air volumes, in exception of the outer roof construction, which is calculated in WUFI1D. The advantages of separating the hygrothermal system between two different tools are many, though there are also some important drawbacks that must be considered.

WUFI1D allows realistic calculation of the transient hygrothermal behavior of building components and contains a wide range of building material properties. This tool is also developed to include all the transfer coefficients that are expected at an exterior surface with relation to the exterior climate and incident solar radiation. A disadvantage with WUFI1D is that it is lacking the capability to include radiation heat exchange in intermediate air spaces or at an interior surface and it is not capable of calculating indoor boundary conditions. In attics, the radiation heat exchange between the interior surfaces may have great influence on the attic environment (Hagentoft et al. 2008). Instead, this radiative interaction and the heat and water vapor transfer that exist below the roof construction, such as the HVAC system, natural and forced convection, thermal conductivity, and water vapor transfer due to convection and diffusion, are simulated in the numerical MATLAB model. Consequently, the numerical tool is designed to simulate the performance of the complete building envelope and inner environment, except for the roof construction, whose hygrothermal performance is instead simulated in WUFI1D. However, since WUFI1D is a one-dimensional hygrothermal tool, the complete attic model requires two WUFI models: one left and one right roof construction. This approach requires an iterative process between these two WUFI1D models and the mathematical MATLAB model, as shown in Figure 1. An iterative simulation process is essential to enable the two WUFI models and the mathematical model to represent a complete and realistic system of the attic space and the adjacent roof construction, which consequently includes the coupling of the simulated elements of WUFI and the attic environment. A thorough description of the mathematical MATLAB model is given in the appendix.

There is a large number of material, geometrical, and system features that must be implemented into a simulation model. This information is obtained either by measurements, from previous simulations, or from standards. All input data for the simulations are intended to represent realistic and true values and not design values, excepting the varying parameters, for which upper values may be taken from design criteria.

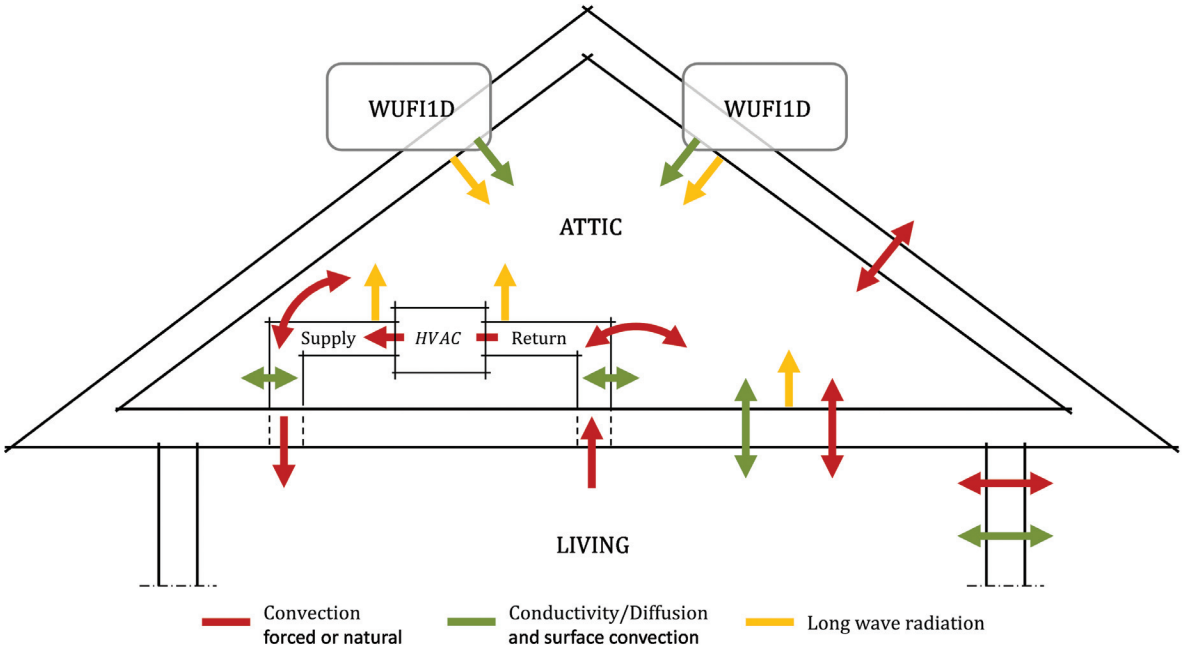

Figure 1 *The unvented attic, hosting an HVAC system, must be considered as a very complex hygrothermal system with a large number of interacting mechanisms. The arrows depict the location and direction of both the heat and water vapor transfer of convection, conductivity/diffusion, and longwave radiation.*

SIMULATION INPUT DATA

There is an extensive amount of information needed if we are expecting a realistic result from running simulations of the unvented attic. This information is used as inputs for the simulation model, of which the most essential are defined in this section.

The air distribution system, applied to the simulation model, is designed as a whole-house air distribution system with intermittent supply and with an exterior air intake on the return side of the HVAC system. The electrical efficiency of the HVAC unit is used to determine the thermal load in the attic. Assuming 90% efficiency results in 10% excess of heat, based on the power needed by the HVAC unit. The airflow rate is determined by the Total Ventilation Rate Method of ANSI/ASHRAE Standard 62.2 (2012), Equations 4.2 and 4.8. The rate of outdoor air exchange in the HVAC system is set to a minimum of 10%, as shown in Table 1. If this rate of fresh air doesn't meet the required minimum outdoor air exchange (ASHRAE 2012) in Equation 4.1, instead the rest is assumed to be fulfilled by infiltration through the building envelope.

The cycling of the HVAC system depends on the indoor temperature and the setpoint temperatures of the thermostat. The setpoint temperatures are usually chosen based on the desired indoor comfort temperatures of the occupants in a building and may vary greatly. The simulation model is designed to optimize the HVAC unit to a 50% on and off cycle at a small span of setpoint temperatures, 70°F/74°F (21.1°C/23.3°C). The cycling is adjusted with the supply airflow rate,

Table 1. Some of the Information Needed to Perform Simulations of the Unvented Attic

Simulation Input Data	
Geometric	
Dimensions of building	33 × 49 ft (10 × 15 m)
Indoor height	8 ft (2.4 m)
Roof slope	20°
Number of bedrooms	4
Number of floors	2
Fenestration area	15% of wall area
HVAC	
Electrical efficiency	90%
Duct length (Ø 10 in./0.25 m)	230 ft/2000 ft^2 of FFA* (70 m/610 m^2 of FFA)
Ratio of supply vs. return ducts	2
Supply duct insulation	R-5 (ft^2·h·°F)/Btu (R=0.88 [m^2·K]/W)
Duct insulation emissivity, ε	0.10
Ratio of fresh air	≥10%
Supply temperature—Cooling	55°F (12.8°C)
Supply temperature—Heating	105°F (40.6°C)

* FFA = finished floor area. The presented ratio is an empirical value based on experience, thus subjectively chosen.

though the rate never falls below the required minimum airflow rate (ASHRAE 2012).

In order to determine the attic temperature, the indoor temperature and the cycling of the HVAC system must be estimated. The indoor thermal conditions mainly depend on thermostat setpoint temperatures, outdoor temperature together with the U-factor of the building envelope, indoor thermal inertia, fenestration area coupled with incident solar radiation, and indoor thermal load. These parameters must be established, with values are based on standards and handbooks:

- The U-factors of the walls, slab on grade, windows, and doors in the simulation model agree with the equivalent U-factors required by the *International Energy Conservation Code* (ICC 2011), Table R402.1.3.
- The indoor thermal inertia from furniture and contents is based on the values presented in ANSI/ASHRAE Standard 90.2 (2007), Section 8.8.2. The thermal inertia inside the attic space is defined by the wooden joists and rafters.
- The indoor thermal load from lights, people, and equipment coincides with Equations 30 and 31 of *ASHRAE Handbook—Fundamentals* (2005), whereas the distribution of the thermal load during the day is based on a Daily Internal Heat Gain Profile (ASHRAE 2007), Table 8.8.1.

With respect to water vapor transfer, the moisture buffering capacity of the materials inside the attic and the indoor space are equivalent with the defined materials with heat capacity. All other material properties are provided from the WUFI material database.

The roof construction, simulated in WUFI1D, is assumed to have an upper covering with shingles, applied on an oriented strand board (OSB) sheathing and with an underlying insulation material of a spray polyurethane foam (SPF). The shingles are assumed to be watertight and have a vapor permeance of 0.3 perm (sd = 10 m). A possible mechanism of solar-driven moisture between the laps of the shingles (Rudd 2005) is not taken into account in this study because of the lack of knowledge and data describing this possible phenomenon.

VARYING PARAMETERS

The varying parameters are chosen based on an importance sampling scheme (Vose 2008), in which the chosen values mostly represent the extreme tail of the parameters' variability. Six different input parameters are selected to vary in the simulation model due to their assumed high influence on the hygrothermal performance of the attic and roof construction. The varying parameters of this study are the following:

- Thermostat setpoint temperatures
- Outdoor climate
- Vapor permeance of the rigid spray foam insulation
- Air leakage rate from supply and return ducts
- Airtightness of ceiling floor
- Indoor moisture production

The thermostat setpoint temperatures are chosen to vary between 70°F/74°F (21.1°C/23.3°C) and 68°F/78°F (20°C/25.6°C), thus representing an assumed small and wide range of, according to the occupants, acceptable indoor temperatures. Practically, the simulation model determines the HVAC cycling based on 70°F/74°F and then applies the same supply airflow rate on 68°/78°F setpoints. This approach will determine the impact on the hygrothermal performance of the unvented attic due to the occupants' desired comfort temperatures.

The outdoor climates, applied to the simulation model, represent U.S. climate zones 1 to 7. The corresponding cities for each climate zone presented in given order are: Miami, FL; Austin, TX; Atlanta, GA; Baltimore, MD; Chicago, IL; Minneapolis, MN; and Fargo, ND.

The thermal resistance of the roof consists of either open- or closed-cell SPF with no assumed coating. The water vapor permeance (diffusion resistance factor) for the open and closed SPFs are 55.1 U.S. perm·in. (μ-value = 2.38) and 1.47 U.S. perm·in. (μ-value = 88.93), respectively. The required thickness, or actually the R-value, of the SPF depends on which U.S. climate zone the roof is to be constructed in and varies between R-30 and R-49 (5.28 and 8.63 m^2·K/W). The R-values are in compliance with regulation (ICC 2011) and implemented into the simulation model.

The unintended air leakages from the air distribution duct system into the attic space can be up to 20% or more (Lstiburek 2006; Polly et al. 2011). Though there are no requirements for duct airtightness if the air-handling unit and ducts are located inside the thermal envelope (ICC 2011), low and high leakage rates are still applied in the simulations to study the effect of different duct leakage rates. In this study, a 4% air leakage of the actual supply and return airflow rates is considered a low leakage rate; a high rate is considered 20%.

A leaky ceiling floor will enable air to exchange between the attic and the living space. The potential air movements are induced by air pressure differences, and the amount of air and the direction of the flow depends on the reigning conditions of temperatures, the ventilation system, or wind forces. Naturally, there are no regulations for the airtightness of the ceiling floor when the attic is located inside the thermal envelope. However, the impact of this phenomenon on the hygrothermal performance of the unvented attic is chosen to be investigated. The airtightness of the ceiling can vary greatly depending on the presence of recessed canister lights and other ceiling penetrations (Rudd 2005). In this study, two assumed conditions are chosen for the ceiling airtightness along the ceiling floor area (CFA): a low value is set to 0.4 cfm50/CFA (2.0 l/[s·m^2]) and a high value is considered 2.0 cfm50/CFA (10.0 l/[s·m^2]). Unpublished measurements made of the ceiling airtightness in a two-story residential building with an unvented attic in Knoxville, TN, USA, resulted in a cfm50/CFA of 1.04 (5.3 l/[s·m^2]). This measured value of cfm50 coincides with the ranges chosen for the simulation model.

The generation of moisture inside a residential building can vary significantly (Christian and Trechsel 1994; Kalamees et al. 2006) depending on the user behavior and household composition and the number and type of appliances and their frequency of use (Yik et al. 2004). Two different moisture production rates are chosen, an average daily rate of 15.8 lb/day (7.2 kg/day) and a high rate of 33.6 lb/day (15 kg/day). The lower value represents a likely daily average of moisture production, based on simulations (Pallin 2012). The upper value agrees with the Residential Design Moisture Generation Rate of ANSI/ASHRAE Standard 160 (2011), Table 4.3.2, for a four-bedroom living space. The moisture production rate varies during the day, depending on the presence and frequencies of moisture-generative activities inside the household. In this study, the daily variation of the moisture production rate is estimated to follow the activity pattern according to the Daily Internal Heat Gain Profile of ASHRAE Standard 90.2 (2007), Table 8.8.1.

Combining all the above varying parameters results in 224 (i.e., $2 \times 7 \times 2 \times 2 \times 2 \times 2$) different scenarios of the unvented attic, where each scenario requires an iterative simulation run with the numerical MATLAB model and the two WUFI1D models. Each scenario is simulated until convergence criteria are fulfilled, in comparison with previous iteration; see Equations A.1 to A.2 in the appendix for details.

RESULT

After completing the simulations of the 224 different scenarios of unvented attics, the following measures of hygrothermal performances were taken into consideration: the variation of the moisture content (MC) in the OSB roof sheathing and the energy demand of the air-handling unit—and also identification of the most reliable and risky compositions of the varying parameters, in terms of the previously described performances.

The MC is a common performance indicator when estimating the service life of a wood-based building material (Straube et al., 2010). Commonly, a MC of 20%–25% is taken as critical upper limit to prevent decay of wooden materials (DIN 2012).The Mold Growth Index (MGI) is also a useful indicator when analyzing the condition of a wood-based material (Ojanen et al. 2011) and estimates the development of mold on a surface depending on the temperature and time of critical RH. In terms of an OSB sheathing with a closely attached upper shingle covering and with an underlying SPF, the surface exposure is very limited; hence, the issue of mold on the OSB surface is questionable. Instead, the MC is used as the performance indicator for moisture safety in this study.

There is a large disparity in the annual development of the MCs for the 224 different simulated OSB sheathings, as shown in Figure 2. Most of the OSB sheathings vary between

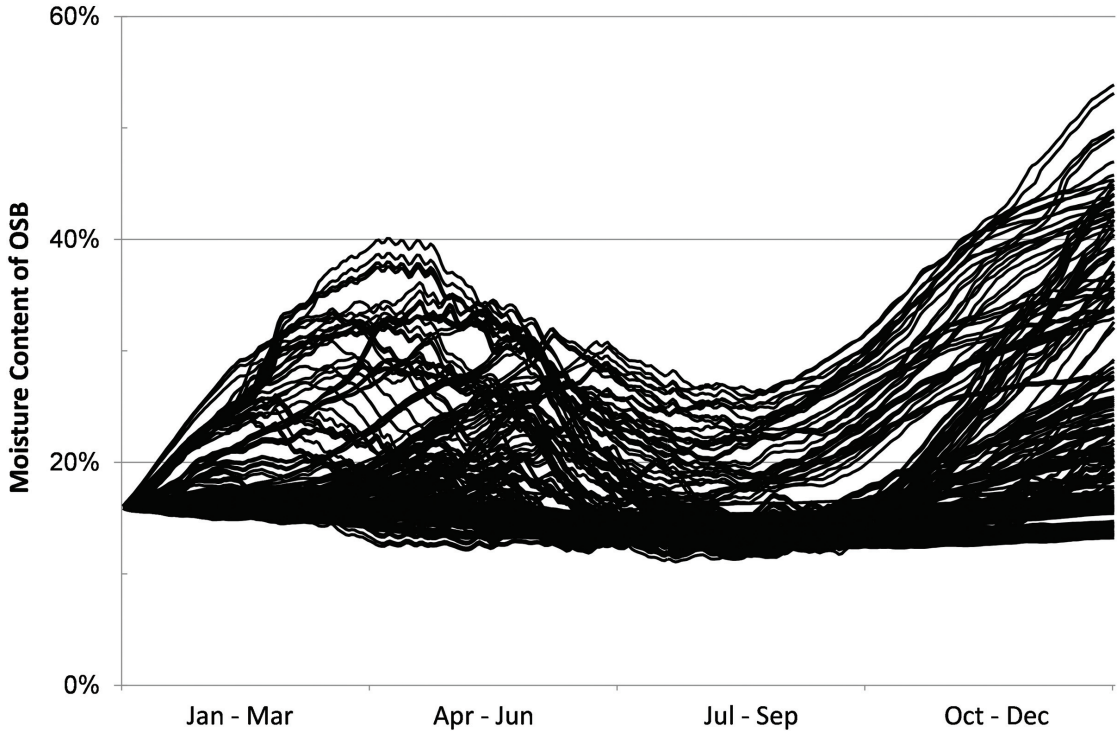

Figure 2 *Annual variation of the MCs in the OSB roof sheathing. The different curves depict the 224 different simulated scenarios of the OSB, including all varying parameters. According to the results, the MCs for most of the OSB sheathings vary between 13% and 17%, though several simulated scenarios result in critical levels of MC in terms of deterioration/rot and must be considered roof constructions with unacceptable hygrothermal performances.*

MCs of 13% and 17% annually; still, there are cases where the MC reaches high above accepted levels. The reason behind the assumed failure of these simulated OSBs is the composition of the varying parameters.

The composition of the parameters for the most reliable and the most risky roof constructions due to critical levels of MC are presented in Table 2. The different scenarios are presented for U.S. climate zones 1 to 7. There are some clear conclusions to make out of Table 2; e.g., every best-performing unvented attic roof is constructed with a closed SPF and with a low indoor moisture supply. The opposite is true for the most risky roof. In all cases, except for climate zone 4, a high duct leakage has a positive effect on the MC of the OSB, most likely due to the dehumidifying effect of the HVAC cooling coils, which, by a higher rate of air leakage, will have a higher influence on the vapor content of the attic air during the operating cooling mode. There are no clear patterns for the varying parameters of the thermostat setpoint temperatures and the ceiling airtightness. A detailed illustration of the annual variation of the MCs is presented in Figure 3 for climate zones 1 and 3, for the simulated best and worst scenarios according to Table 2.

The importance of the different varying parameters on the maximum MC of the OSB sheathing can be estimated with a sensitivity analysis. Since the values of the varying parameters are chosen based on their importance and not their likeliness of occurrence, the sensitivity analysis is not probabilistic and should therefore not be considered such. A common analysis method to compare the impact of varying input parameters on the result is to apply an Importance Index (Hamby 1994), which takes into account the variances of the parameters on the chosen indicator. This study uses a similar approach, in which the importance of the different varying parameters is estimated by measuring the average deviation of a varying parameter when remaining all parameters but one are fixed. Repeatedly, the disparity in the annual maximum of MC is compared when changing only the value of the investigated parameter. The average disparity of the parameter (in this study the MC) is referred to as D_p and expressed as follows:

$$D_p = \frac{1}{n/2} \sum_{i=1}^{n/2} \left| X_{i,p}^{A} - X_{i,p}^{B} \right| \quad (1)$$

$$\text{for } A \in C,\ B \in C,\ A = -B$$

where

D_p = average disparity of one varying parameter, p (p = 1:6)

X = indicator or the analysis (in this case the maximum MC), %

n = total number of compositions, i.e., sets of different values of X (n = 224)

A is one of n compositions of the varying parameter, B is the opposite of A due to the chosen parameter p, and C is the set of all n compositions of varying parameters.

As an example, if a parameter p = 3 is varying in a binary sequence and A = 010110, then B = 011110 because B is considered the opposite of A in the position of the third parameter. In the case of this study, an example is the following: if we considered the importance of the moisture production, we'll look at the maximum MC of the first simulated scenario. Then we're comparing it with the MC in the simulated scenario where all the parameters are the same, except for the moisture production. We then summarize the disparities of the maximum MC when moving along all the simulated scenarios, where A is the scenario we are comparing with B. For an analysis with n = 224 simulated scenarios, D_p is based on the n/2 number of differences in MC; otherwise, a specific relative disparity is used twice, i.e., when the previous sequence of B becomes A.

Furthermore, D_p for each varying parameter is weighted with the parameter with the highest value, referred to as D_p^{max}; hence an relative disparity, D_p^{rel}, can be defined for each parameter as:

$$D_p^{rel} = \frac{D_p}{D_p^{max}} \quad (2)$$

Consequently, the parameter with the highest D_p obtains a maximum relative value of 1.0. All other parameters receive a D_p^{rel} of either 1.0 or lower. This method enables a comparison of the varying parameters on their influence on a chosen performance indicator, which in this study is the maximum MC of the OSB sheathing for a simulated consecutive year, as presented in Figure 4. According to the analysis, the vapor permeance of the SPF is of greatest importance on the MC of the OSB—meaning, whether the SPF is closed or open, it will have the highest influence on the estimated conditions of the OSB sheathing in the roof construction. Other important parameters are the climate and the indoor moisture production. In this study, the chosen variation of the indoor moisture production was set to vary between a normal and high excess of moisture. If an expected lower value of the moisture production were been used instead (as for the duct leakage, the setpoint temperatures, and the ceiling airtightness), instead a larger value of D_p^{rel} would have been expected.

There is a low influence on the maximum MC of the OSB in terms of the thermostat setpoint temperatures and duct leakages, though the duct leakage seems to have some influence according to Table 2. However, these varying parameters must be assumed to possess a larger impact on the energy demand of the HVAC unit. Naturally, the thermostat setpoint temperatures govern the cycling of the HVAC and therefore the amount of energy required. Figure 5 illustrates the decrease in energy loss of the HVAC unit when changing the setpoint temperatures from 70°F/74°F (21.1°C/23.3°C) to 68°F/78°F

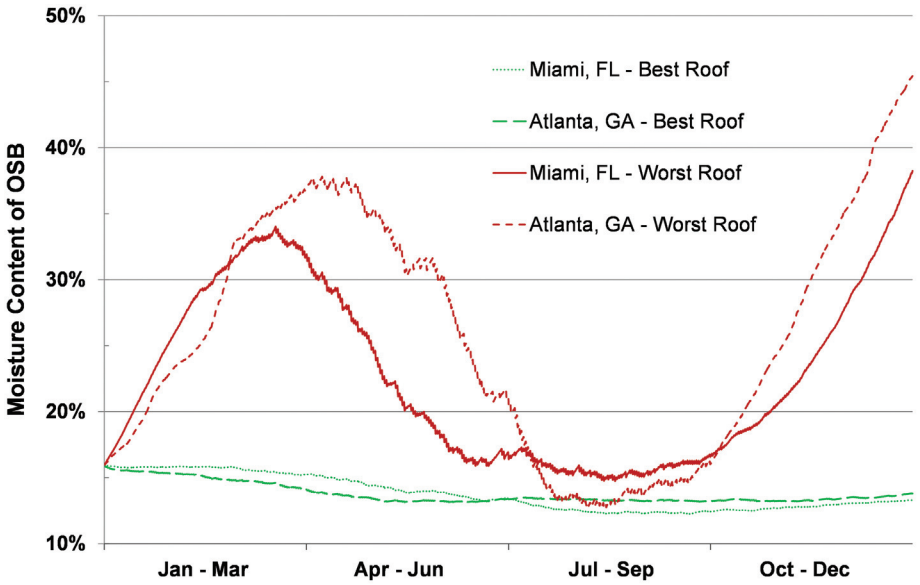

Figure 3 *The annual accumulation of moisture content (MC) in the OSB sheathing, for the best and worst simulated scenarios and for the chosen cities of U.S. climate zones 1 and 3. In the two OSB sheathings with the lowest accumulation of moisture, the end value is lower than the start value, which indicates that the MC must be assumed to decrease further if simulated for a longer period of time.*

Table 2. Compositions of the Varying Parameters with Lowest and Highest Risk of Deterioration of the OSB due to the End Value of MC, Presented for U.S. Climate Zones 1 to 7. In the Simulation, the Starting Value of the OSB MC is 16%.

Rank	Climate Zone	Direction	Setpoint	SPF	Duct Leakage	Ceiling Leakage	Moisture Production	MC End Value
Best	1	South	70/74	Closed	20%	2@50	Normal	14%
Worst		North	68/78	Open	4%	10@50	High	38%
Best	2	South	70/74	Closed	20%	2@50	Normal	13%
Worst		North	70/74	Open	4%	10@50	High	43%
Best	3	South	70/74	Closed	20%	2@50	Normal	13%
Worst		North	68/78	Open	4%	10@50	High	45%
Best	4	South	68/78	Closed	4%	10@50	Normal	14%
Worst		North	68/78	Open	4%	10@50	High	54%
Best	5	South	70/74	Closed	20%	2@50	Normal	14%
Worst		North	68/78	Open	4%	10@50	High	47%
Best	6	South	70/74	Closed	20%	2@50	Normal	14%
Worst		North	68/78	Open	4%	10@50	High	45%
Best	7	South	68/78	Closed	20%	2@50	Normal	13%
Worst		North	68/78	Open	4%	10@50	High	37%

(20°C/25.6°C). The analysis does not take the efficiency of the HVAC unit into consideration, nor the differences between heating and cooling; it solely considers the amount of energy needed, in a thermodynamic matter, to either cool or heat the air that is supplied into the living area. In this study, we refer

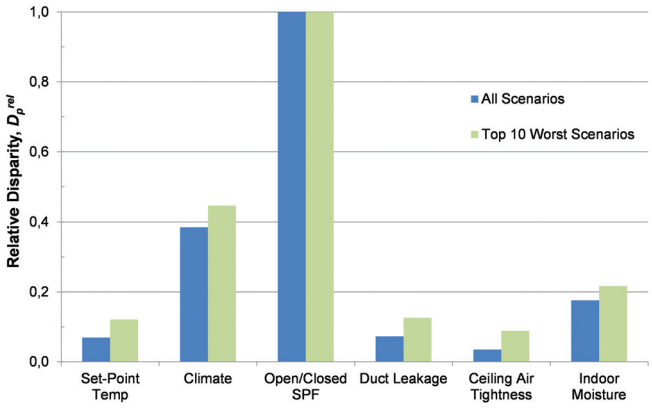

Figure 4 *The relative disparity, D_p^{rel}, for the varying parameters of this study. According to the analysis, the simulated maximum MC of the OSB will vary mostly depending on weather the SPF is vapor closed or open. Both the climate and the indoor moisture production will have rather high influence as well.*

to the reduced amount of energy as a factor of reduction (F_{red}) and express it as follows:

$$F_{red} = \frac{1}{n/2} \sum_{i=1}^{n/2} \frac{Q^B_{heating,n} + Q^B_{cooling,n}}{Q^A_{heating,n} + Q^A_{cooling,n}} \qquad (3)$$

where

$Q_{heating}$ = energy required to heat the supply air to 105°F (40.6°C)

$Q_{cooling}$ = energy required to cool the supply air to 55°F (12.8°C), in which n, A, and B equal the definitions of Equation 1

Once again, simulation A represents the investigated scenario that is compared with the scenario where all parameters are fixed except for the setpoint temperatures, i.e., simulation B. Therefore A means the scenario with a setpoint of 70°F/74°F (21.1°C/23.3°C) and B means 68°F/78°F (20°C/25.6°C). A value of F_{red} close to zero means a low energy reduction if changing the range of indoor comfort temperatures.

The analyses of the F_{red} for the different U.S. climate zones are presented in Figure 5, which indicates that a warmer climate has a higher potential of energy savings compared to a colder climate. It is important to emphasize that the U.S. climate zones can only be compared with each other as relative reductions, e.g., a specific amount of energy in a 20% savings for one climate zone can actually be larger than a 30% savings for another.

The duct leakages from the air distribution system also prove to influence the cycling of the HVAC unit. Figure 6 illustrates the increase in energy demand of the HVAC unit when changing the assumed leakage rate from 4% to 20% in the supply and return duct system. As for the previous analysis with the setpoint temperatures, the efficiency of the HVAC unit is not taken into consideration, nor are the differences between heating and cooling. In comparison with the reduction of energy in Equation 3, the reduction becomes an increase since the relative difference in energy demand is instead referred to as F_{inc}.

The result of the analysis in Figure 6 shows that the leakage rate of the duct system does make a difference on the annual energy cost (AEC), despite the lack of regulations for

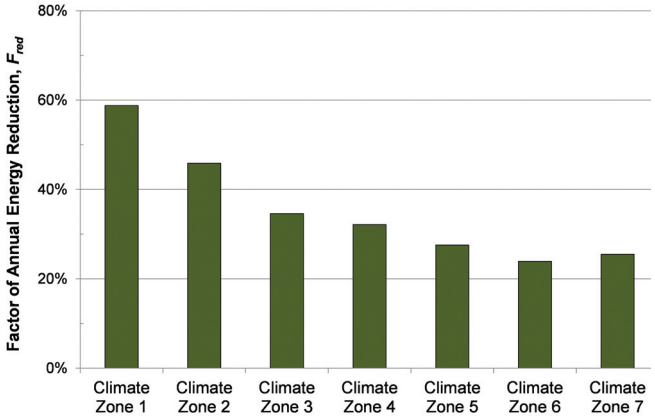

Figure 5 *Relative annual reduction of energy demand when changing the thermostat setpoint temperatures from 70°F/74°F (21.1°C/23.3°C) to 68°F/78°F (20°C/25.6°C). According to the results, warmer climate zones have a higher savings potential in HVAC energy demand if a wider range in setpoint temperatures is accepted.*

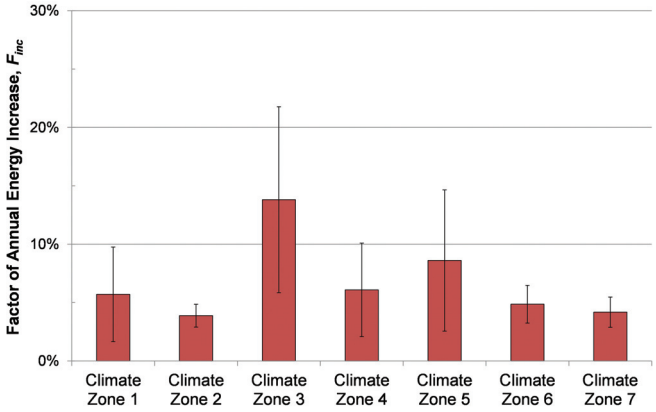

Figure 6 *Relative annual increase of energy demand when changing the assumed ventilation duct leakage from 4% to 20%. The results are presented for U.S. climate zones 1 to 7, where the increases will vary from 5% to 14%. A large uncertainty must be expected, as defined by the error bars, whose values represent the standard deviation.*

the airtightness of the duct system when situated inside the thermal envelope (ICC 2011, Section R.403.2.2) or accounted for (ASHRAE 2007, Section 8.8.4.5). The relative increase in energy required to heat or cool the air varies between 5% and 14% when comparing a 4% duct leakage with a 20% leakage rate, though with a large uncertainty, as seen in Figure 6.

Furthermore, the RH inside the attic was investigated due to the risk of mold growth. All of the 224 simulated unvented attics received nothing else than an index of zero on the MGI, which means that none of the simulated attic climates had any potential of developing mold on wood-based surfaces inside the attic. This result was expected since an unvented attic is embraced by the thermal envelope, but this result was nonetheless important for the verification of the simulation model. Therefore, the risk of decay in the OSB sheathing is considered most important in terms of moisture safety; thus, mold growth inside the attic space becomes less important.

CONCLUSION

In this study, 224 different compositions with 6 varying parameters were simulated for an unvented attic and the adjacent roof construction. The six varying parameters are the thermostat setpoint temperatures, the outdoor climate, the vapor permeance of the rigid spray foam insulation, the air leakage rate from the ventilation supply and return ducts, the airtightness of the ceiling floor, and the indoor moisture production. The impact due to the parameter variability on the hygrothermal performance of the roof and attic was investigated. Three different performance indicators were analyzed: the maximum moisture content (MC) of the OSB, the HVAC system energy demand, and the mold growth index (MGI) of the wood-based materials inside the attic space.

The MC in the OSB sheathing varies mostly due to whether the spray polyurethane foam (SPF) is vapor closed or open. Having an open SPF is actually a risk in all the investigated U.S. climate zones, 1 to 7, depending on the chosen values of the other varying parameters. Naturally, the outdoor climate will influence the MC of the OSB, but also the indoor moisture production rate has a significant impact.

A high air leakage rate from the air distribution duct system has a positive impact on the MC of the OSB sheathings due to the dehumidifying effect of the HVAC unit, though it has a negative influence in terms of the HVAC energy demand. On average, an increase in 5% to 14% in energy demand is predicted for the different climate zones when comparing a 4% with a 20% duct leakage rate, though both a higher and a lower increase can be expected. Consequently, this study shows that the rate of air leakage from the ventilation duct system can make a large impact on the annual energy demand of a residential building, despite the lack of any existing guidance or regulations for the airtightness of the duct system when constructed inside the thermal envelope. Furthermore, the thermostat setpoint temperatures have a very large impact on the annual energy demand. Changing from 70°F/74°F (21.1°C/23.3°C) to 68°F/78°F (20°C/25.6°C) has the highest impact in hotter climates, but colder climates also have a significant decrease in energy demand when accepting a wider span of setpoint temperatures.

The risk of developing mold on surfaces inside the attic space is negligible for all the simulated plausible cases of an unvented attic. However, it is important to emphasize that the outer roof construction is assumed to be airtight in the simulation model and that any deviation from that assumption will affect the risk of mold inside the attic space.

Finally, this study proves that a moisture-safe unvented roof can be constructed for each U.S. climate zone. A parameter study has shown which of the parameters has the largest impact on the hygrothermal performance, as illustrated in Figures 4 to 6, and which alternatives exist to improve the performances; see Table 2. Generally, a closed SPF is a good decision in terms of the risk of moisture damage in the OSB. The roof shingle system of the simulated roof construction is simulated watertight and with a rather high vapor permeance. A possible mechanism of solar-driven moisture between the laps of the shingles is therefore not taken into account. However, recent unpublished measurements at multiple Oak Ridge National Laboratory (ORNL) test facilities indicate that moisture transport through the roof shingle system is suspected. It is also important to point out the risk when enclosing an organic material, such as the OSB, between two rather vaportight materials such as the SPF and the roof shingles. If water or vapor reaches the OSB sheathing, the drying potential is very low and the moisture becomes trapped. This possible event has not been investigated in this study, though it should be considered as a potential risk that ought to be further studied. Minimizing the moisture-productive activities and appliances inside the living space may also be effective to increase the moisture safety of the OSB. With regards to energy, the setpoint temperatures accepted by the occupants and the reduced air leakages from the ventilation duct system make a significant difference on the HVAC system energy demand.

APPENDIX

In this appendix, a detailed description is given of the structure, mathematical expressions, iterative process, and convergence criteria behind the numerical MATLAB model of the studied roof construction. The description is divided into two parts: one for the heat transfer and one for the water vapor transfer, representing the hygrothermal performance if the complete unvented roof construction. The relations between temperatures/vapor contents and incident heat/moisture sources can be defined in a network scheme, where each node represents a temperature/vapor content, connected to each other with conductances. The thermal network, representing the heat transfer of the unvented attic, is illustrated in Figure 7, and the network representing the water vapor transfer is presented in Figure 9.

Nomenclature

Temperatures, K

T_e = outdoor air temperature

T_{in} = indoor air temperature

T_{attic} = attic air temperature

T_{supply} = ventilation supply air temperature

T_{return} = ventilation supply return air temperature

T_n = temperature at surface n

T_N^{fict} = fictitious radiation node temperature at node N

Conductance—Conductivity, W/K

K_{cond}^{duct} = heat conductance between the inner and outer ventilation duct surfaces

$$= \frac{2 \cdot \pi \cdot \lambda_{duct} \cdot L_{duct}}{\ln(r_2/r_1)}$$

where

λ_{duct} = thermal conductivity of the duct insulation

L_{duct} = total length of the ventilation ducts

r_2 = outer radius

r_1 = inner radius

$K_{cond}^{wall+slab}$ = mutual conductance of the thermal conductivity between the interior and exterior surfaces of the building envelope, except through the ceiling and the roof

K_{cond}^{ceil} = conductance, representing the heat conductivity between the upper and lower ceiling surfaces

Conductance—Convection, W/K

$K_{conv}^{sr,\,n}$ = conductance from natural convection at an interior surface n

$$= 2 \cdot \sqrt[3]{T_a - T_s} \cdot A_s$$

where

T_a = ambient air temperature

T_s = surface temperature

A_s = area of surface n

$K_{conv}^{leak,\,ceil}$ = natural air convection-induced conductance between the indoor living and the attic space

$$= \rho_{air} \cdot c_{air} \cdot C \cdot \Delta P^{\exp}$$

where

C = air leakage coefficient

ΔP = convective induced pressure difference

exp = air pressure exponent

and

$$\Delta P = z \cdot 3456\left(\frac{1}{T_{attic}} - \frac{1}{T_{in}}\right),$$

in which z is the vertical distance from the neutral pressure plane. ΔP can either be positive or negative, depending on the direction of the airflow.

$K_{conv}^{leak,\,c}$ = natural air convection-induced conductance, through building component c; see $K_{conv}^{leak,\,ceil}$ for computational methods

K_{airing} = forced-air convection due to airing, regulated by the occupants of the building

$K^{vent,\,supp}$, $K^{vent,\,ret}$ = heat conductances as a result of the mechanically induced air movements from and to the HVAC system

$K_{leak}^{vent,\,sup}$ = conductance due to air leakages in the supply duct system

$K_{inner}^{vent,\,ret}$ = exiting airflow conductance, from the inside into the return duct system

$K_{leak\ attic}^{vent,\,ret}$ = conductance due to air leakages from the attic and into the return duct system

$K^{vent,\,fresh}$ = conductance, representing the supplied outdoor air into the HVAC system

Conductance—Radiation, W/K

$K_{rad}^{sr\_n}$ = radiative surface conductance at surface n.

$$= \frac{\varepsilon_n \cdot A_n}{1 - \varepsilon_n} \cdot \sigma \cdot 4 \cdot T_n^3$$

where

A_n = surface area of n

ε = surface emissivity

σ = Stefan-Boltzmann constant

K_{rad}^{nm} = conductance between fictitious radiative temperature nodes m and n

$$= A_n \cdot F_{nm} \cdot \sigma \cdot 4 \cdot \bar{T}_{nm}^3$$

where

F_{nm} = view factor from surface n to m

$\bar{T}_{nm}$ = average surface temperature of n and m

Heat Sources, W

I_{unit}^{HVAC} = excess of heat from the operating HVAC unit, acting as a heat source into the attic space

I_{pwr}^{HVAC} = power needed to heat or cool the air to a given supply temperature

I_{in} = heat load from indoor activities, appliances, and humans

The symbols for water vapor transfer are similar to those for heat transfer. In general, T is substituted with v, which is the volumetric vapor content, and K is replaced by Kv, which is the conductance for water vapor transfer. There are two additional symbols defined in the following subsection.

Moisture Sources and Sinks, lb (kg)

G_{in} = moisture load from indoor activities, appliances, and humans

S = reduction of moisture content in the supply air due to the dehumidifying effect of the cooling coils

Heat and moisture balances are calculated for each temperature and vapor node and for each given time step. The simulation model is programmed in a mathematical numerical tool, representing the complete building except for the roof construction. The numerical tool calls on WUFI1D, subsequently representing the roof construction. In order to make these two separate models work, an iterative process is required since the output parameters of one model serve as the input parameters of the other. The iterations continue until two convergence criteria are fulfilled. In this study the required convergences are 0.1% for the attic temperature and 1% for the vapor content of the attic air. These convergences are referred to as C_{temp} and C_{moist}, then:

$$C_{temp}^{max} \leq \frac{T_{attic}(i+1,t) - T_{attic}(i,t)}{T_{attic}(i,t)} \leq 0.1\% \qquad \text{(A.1)}$$

$$C_{moist}^{max} \leq \frac{v_{attic}(i+1,t) - v_{attic}(i,t)}{v_{attic}(i,t)} \leq 1.0\% \qquad \text{(A.2)}$$

for iteration number i and at the time step t. In order to fulfill the convergences, C_{temp} and C_{moist} shall not exceed the criteria for any of the simulated time steps.

Heat Transfer Balances

The temperature of each node is calculated by balancing the flux of energy into the nodes. The temperatures are dependent of each other and therefore determined explicitly, i.e., the computations are based on temperatures from previous simulated time steps. Once the first complete simulation iteration has been finished between the two separate models, the computations are based on the temperatures from the same time step but from the previous iteration. To clarify, the first iteration uses temperatures, when needed, from the previous time step; the subsequent iterations use the temperatures from the present time step but from the previous iteration. This approach is the reason behind the setup for convergences criteria in which the iterations continue until the results from the last two iterations converge.

Figure 7 illustrates the energy balances in the air temperature nodes of the roof and attic models, as shown in Figure 7.

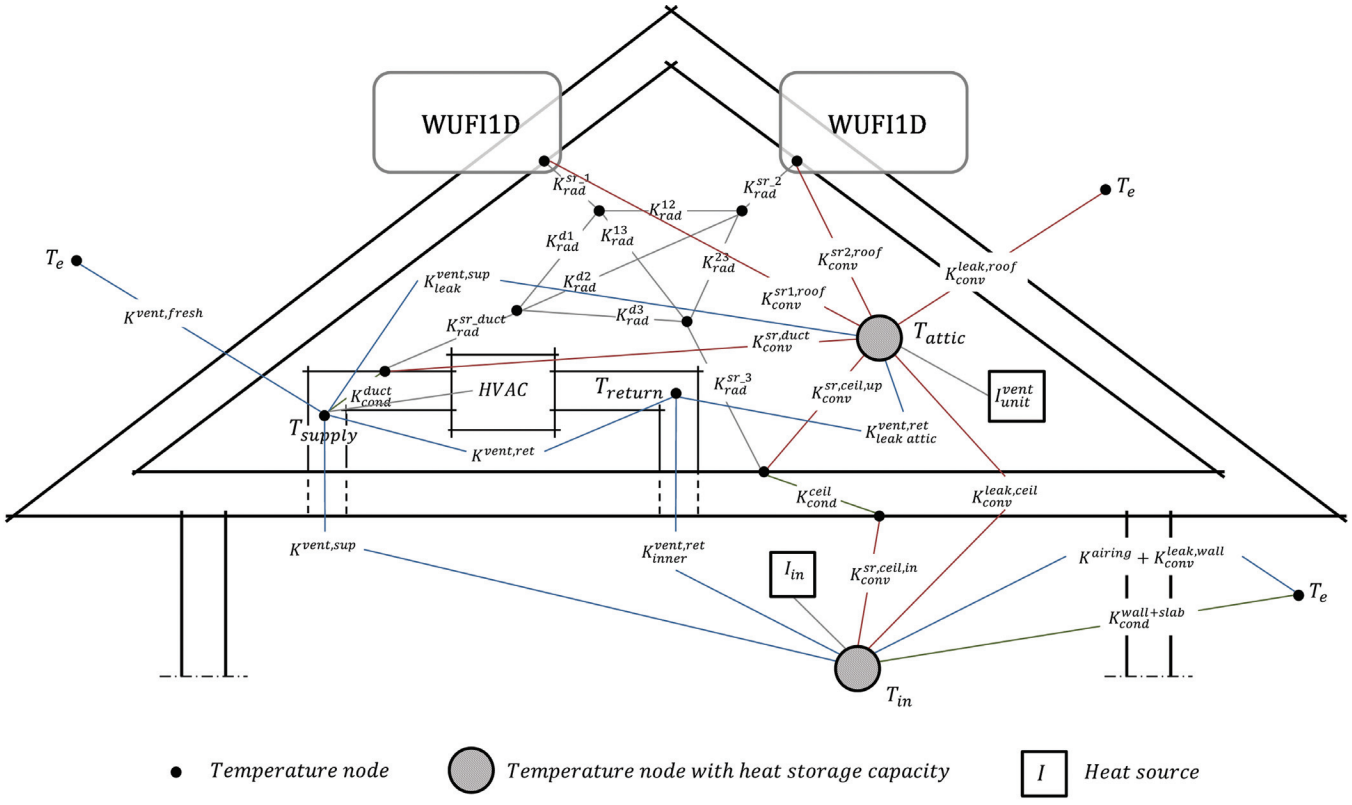

Figure 7 *Thermal network of the unvented attic, representing the overall heat transfer between the attic space, the air distribution system, and the indoor and outdoor environments. Each surface or air temperature is represented as a node, connected to each other with conductances.*

Ventilation Supply and Return Temperatures, T_{supply} and T_{return}

The thermostat setpoint temperatures determine whether the HVAC system is running or not. When the indoor temperature is exceeded by these setpoints, the HVAC system is started. The temperature of the ventilation supply air, T_{supply}, is either 55°F (12.8°C) or 105°F (40.6°C), depending on whether the HVAC unit is in cooling or heating mode. Still, there are unknown temperatures and a heat source involved in the energy balance of T_{supply}, hence a heat transfer network is required:

$$T_{supply} = \frac{\begin{pmatrix} T_{surf}^{duct} \cdot K_{cond}^{duct} + T_{return} \cdot K^{vent,ret} + T_e \\ \cdot K^{vent,fresh} + I_{pwr}^{HVAC} \end{pmatrix}}{K_{supply}} \quad (A.3)$$

in which

$$K_{supply} = K_{cond}^{duct} + K^{vent,ret} + K^{vent,fresh} \quad (A.4)$$

Furthermore, the required power of the HVAC unit, I_{pwr}^{HVAC}, can be expressed as follows:

$$I_{pwr}^{HVAC} = \begin{pmatrix} T_{supply} \cdot K_{supply} - T_{surft}^{duct} \cdot K_{cond}^{duct} \\ - T_{return} \cdot K^{vent,ret} - T_e \cdot K^{vent,fresh} \end{pmatrix} \quad (A.5)$$

where

$$T_{return} = \frac{T_{in} \cdot K_{inner}^{vent,ret} + T_{attic} \cdot K_{leak\ attic}^{vent,ret}}{K_{return}} \quad (A.6)$$

$$K_{return} = K_{inner}^{vent,ret} + K_{leak\ attic}^{vent,ret} \quad (A.7)$$

The Attic Temperature, T_{attic}

The attic temperature is determined by a coupled energy balance and a thermal capacity. In this study, the thermal capacity of the attic consists of the wooden ceiling joists and the air volume of the attic space. The relation between the heat capacity and the energy flux, Q (W), is defined as follows:

$$\frac{dT_{attic}}{dt} \cdot \Sigma(V \cdot \rho \cdot c)_{attic} = Q_{cond+conv} + Q_{Ra} + Q_I \quad (A.8)$$

$$Q_{cond+conv} = \begin{pmatrix} (T_{surf}^{left\ roof} - T_{attic}) \cdot K_{conv}^{sr1,roof} \\ + (T_{surf}^{right\ roof} - T_{attic}) \cdot K_{conv}^{sr2,roof} \\ + (T_{surf}^{ceil,up} - T_{attic}) \cdot K_{conv}^{sr,ceil,up} \\ + (T_{surf}^{duct} - T_{attic}) \cdot K_{conv}^{sr,duct} \end{pmatrix} \quad (A.9)$$

$$Q_{Ra} = \begin{pmatrix} T_{supply} \cdot K_{leak}^{vent,sup} - T_{attic} \cdot K_{leak\ attic}^{vent,ret} \\ + (T_e - T_{attic}) \cdot K_{conv}^{leak,roof} \\ + (T_{in} - T_{attic}) \cdot K_{conv}^{leak,ceil} \end{pmatrix} \quad (A.10)$$

$$Q_I = I_{unit}^{vent} \quad (A.11)$$

If existing, $K_{conv}^{leak,roof}$ and/or $K_{conv}^{leak,ceil}$ are assume to be in a balanced airflow, meaning there is an exchange of equal airflow in both directions.

For a specific time step $t = j, j-1, j+2 \ldots j+n$, the disparity in T_{attic} compared to the previous time step is defined as:

$$(T_{attic}^{j+1} - T_{attic}^{j}) = dt \frac{\begin{pmatrix} (T_{surf}^{left\ roof} - T_{attic}^{j}) \cdot K_{conv}^{sr1,roof} \\ + (T_{surf}^{right\ roof} - T_{attic}^{j}) \cdot K_{conv}^{sr2,roof} \\ + (T_{surf}^{ceil,up} - T_{attic}^{j}) \cdot K_{conv}^{sr,ceil,up} \\ + (T_{surf}^{duct} - T_{attic}^{j}) \cdot K_{conv}^{sr,duct} \\ + T_{supply} \cdot K_{leak}^{vent,sup} - T_{attic}^{j} \\ \cdot K_{leak\ attic}^{vent,ret} + (T_e - T_{attic}) \\ \cdot K_{conv}^{leak,roof} + (T_{in} - T_{attic}) \\ \cdot K_{conv}^{leak,ceil} + I_{unit}^{vent} \end{pmatrix}}{\Sigma(V \cdot \rho \cdot c)_{attic}} \quad (A.12)$$

The Indoor Temperature, T_{in}

The temperature if the indoor environment is also determined by a coupled energy balance with a thermal capacity of the inner mass. The thermal inertia of the indoor environment consists of furniture and contents (ASHRAE 2007, Section 8.8.2) equivalent to the thermal properties of wood and gypsum. The indoor temperature and coupled energy balance is defined as:

$$\frac{dT_{in}}{dt} \cdot \Sigma(V \cdot \rho \cdot c)_{in} = Q_{cond+conv} + Q_{Ra} + Q_I \quad (A.13)$$

where

$$Q_{cond+conv} = (T_{ceil,low}^{sr} - T_{in}) \cdot K_{ceil,low}^{sr} + (T_e - T_{in}) \cdot K_{cond}^{wall+slab} \quad (A.14)$$

$$Q_{Ra} = \begin{pmatrix} T_{supply} \cdot K^{vent,sup} - T_{in} \cdot K_{inner}^{vent,ret} \\ + (T_{attic} - T_{in}) \cdot K_{conv}^{leak,ceil} + (T_e - T_{in}) \\ \cdot (K^{airing} + K_{conv}^{leak,ceil}) \end{pmatrix} \quad (A.15)$$

$$Q_I = I_{in} \tag{A.16}$$

For a specific time step $t = j, j+1, j+2 \ldots j+n$, the disparity in T_{in} compared to the previous time step is defined as:

$$(T_{in}^{j+1} - T_{in}^{j}) = \frac{dt \left(\begin{array}{c} (T_{ceil,\,low}^{sr} - T_{in}) \cdot K_{ceil,\,low}^{sr} \\ + (T_e - T_{in}^{j}) \cdot K_{cond}^{wall+slab} + T_{supply} \\ \cdot K^{vent,\,sup} - T_{in}^{j} \cdot K_{inner}^{vent,\,ret} \\ + (T_{attic} - T_{in}) \cdot K_{conv}^{leak,\,ceil} \\ + (T_e - T_{in}) \cdot (K^{airing} + K_{conv}^{leak,\,ceil}) \\ + I_{in} \end{array} \right)}{\Sigma (V \cdot \rho \cdot c)_{in}} \tag{A.17}$$

Radiation Heat Exchange

The exchange of longwave radiation between the surfaces of the attic will affect not only each other but also all the heat transfer in the attic. The relation between the surfaces in terms of longwave radiation is illustrated in Figure 8.

The fictitious node temperatures, T_1^{fict} to T_4^{fict}, are defined as:

$$T_1^{fict} = T_1 \cdot K_{rad}^{sr_1} + T_2^{fict} \cdot K_{rad}^{12} + T_3^{fict} \cdot K_{rad}^{13} + T_4^{fict} \cdot K_{rad}^{14} \tag{A.18}$$

$$T_2^{fict} = T_2 \cdot K_{rad}^{sr_2} + T_1^{fict} \cdot K_{rad}^{12} + T_3^{fict} \cdot K_{rad}^{13} + T_4^{fict} \cdot K_{rad}^{14} \tag{A.19}$$

$$T_3^{fict} = \ldots$$

Furthermore, the surface temperatures, T_1 to T_4, are derived out of T_1^{fict} to T_4^{fict}. The surface temperature of the return duct system is assumed to be equivalent with the attic temperature; thus it is assumed to be negligible in this study.

Water Vapor Transfer Balances

As for the heat transfer, the vapor content of each node is calculated by balancing the flux into the nodes. The vapor contents are dependent of each other and therefore determined explicitly. Once the first complete simulation iteration between the two separate models has been finished, the computations are based on the vapor contents from the same time step but from the previous iteration, i.e., as the iterations continue, the vapor contents are determined more implicitly. The vapor contents of the supply and return air, v_{supply} and v_{return}, are both calculated based on first explicit then implicit values of the vapor contents of the attic and indoor air, v_{attic} and v_{in}.

Ventilation Supply and Return Air Vapor Content, v_{supply} and v_{return}

From Figure 9:

$$v_{return} = \frac{v_{in} \cdot Kv_{inner}^{vent,\,ret} + v_{attic} \cdot Kv_{leak\ attic}^{vent,\,ret}}{Kv_{return}} \tag{A.20}$$

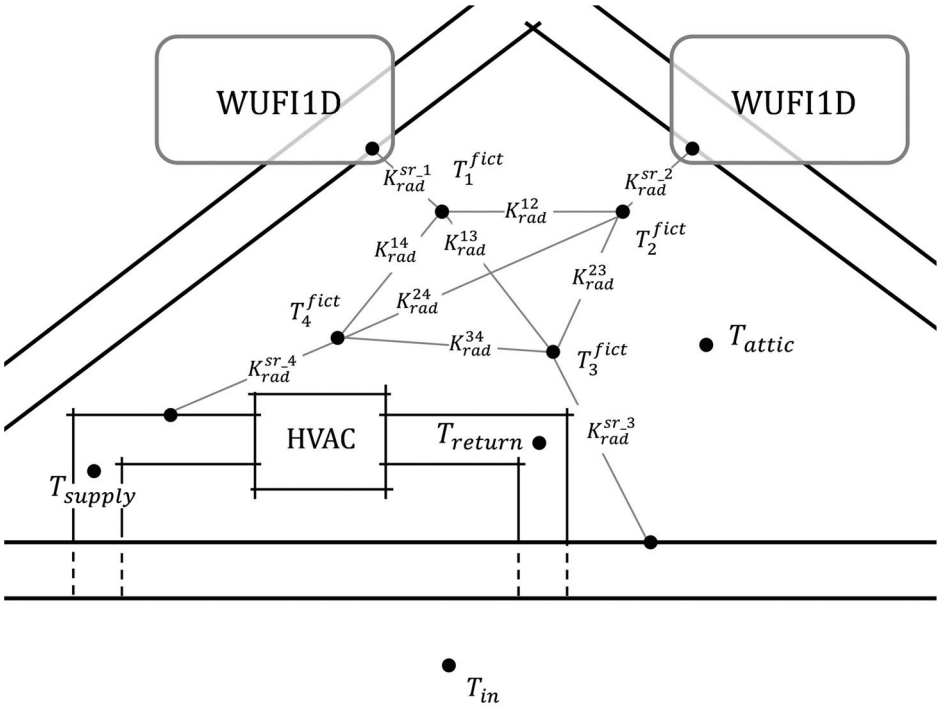

Figure 8 *Longwave radiation heat exchange between the surrounding surfaces of the attic space. The surface temperatures are determined with the help of fictitious node temperatures.*

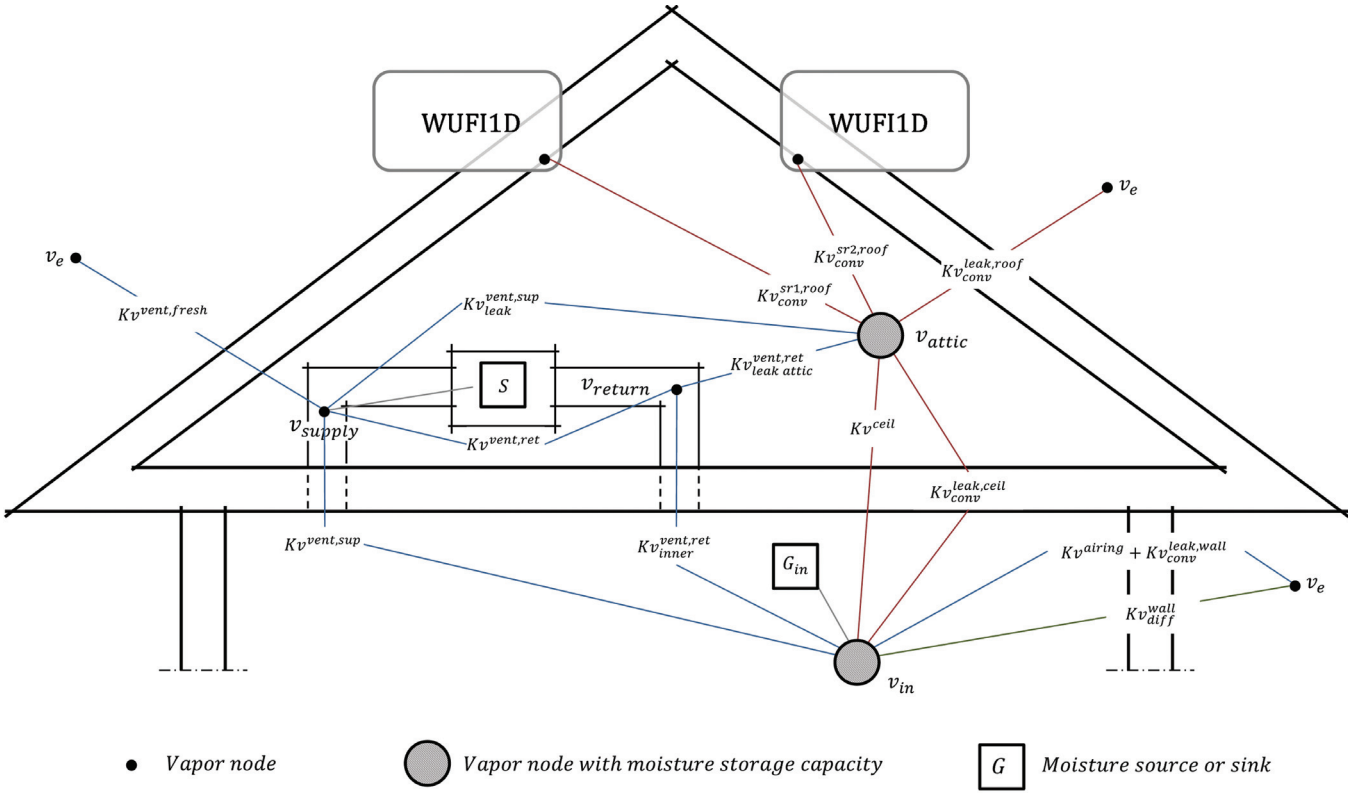

Figure 9 *Network of the unvented attic, representing the overall water vapor transfer between the attic space, the air distribution system, and the indoor and outdoor environments. Each vapor content of a surface or air volume is represented as a node, connected to each other with conductances.*

where

$$Kv_{return} = Kv_{inner}^{vent,ret} + Kv_{leak\ attic}^{vent,ret} \quad \text{(A.21)}$$

and

$$v_{supply} = \frac{v_e \cdot Kv^{vent,fresh} + v_{return} \cdot Kv^{vent,ret}}{Kv_{supply}} \quad \text{(A.22)}$$

where

$$Kv_{supply} = Kv^{vent,fresh} + Kv^{vent,ret} \quad \text{(A.23)}$$

In Figure 10, S represents the reduction of vapor content in the supply air due to the dehumidifying effect of the HVAC cooling coils; therefore, S is only operating when the HVAC system is in cooling mode.

If the HVAC system runs in cooling mode, the following is valid:

$$v_{res,sup} = \frac{v_e \cdot Kv^{vent,fresh} + v_{return} \cdot Kv^{vent,ret}}{Kv_{supply}} \quad \text{(A.24)}$$

$$v_{supply} = v_{res,sup} - S = \left(\frac{v_e \cdot Kv^{vent,fresh} + v_{return} \cdot Kv^{vent,ret}}{Kv_{supply}} \right) - S \quad \text{(A.25)}$$

The dehumidifying effect can be defined as the difference in vapor content between the residual vapor content, $v_{res,sup}$, and the dew point, v_{sat}, at the supplied cooling temperature, T_{supply}:

$$S = (v_{res,sup} - v_{sat}(T_{supply})) \quad \text{(A.26)}$$

Vapor Content of the Attic Air, v_{attic}

The wooden joists, supporting the ceiling floor, are assumed to buffer moisture in which d_e is the effective moisture penetration depth. This effective depth, together with the surface area, defines the moisture buffering volume and increases with increasing periodic time length, t, of varying air humidity:

$$d_e = \sqrt{a_v \cdot t} \quad \text{(A.27)}$$

with a moisture diffusivity a_v.

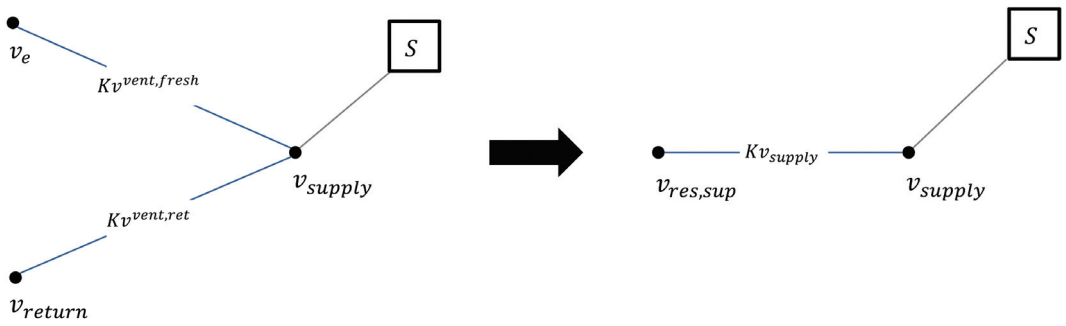

Figure 10 *A network reduction of the ventilation supply and return air vapor contents together with the dehumidifying effect of the HVAC cooling coils,* S.

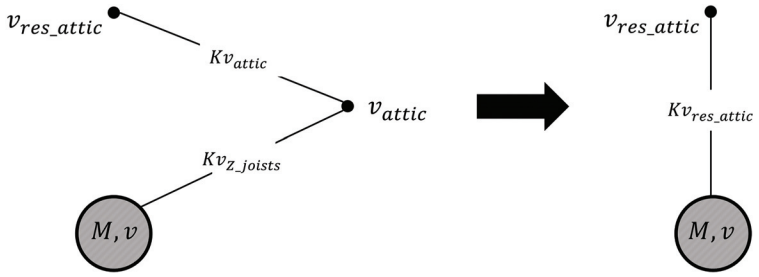

Figure 11 *A network reduction depicting the coupled water vapor transfer and buffering capacity inside the attic space.* M *is the total moisture weight of the buffering material and* v *is the vapor content.*

The coupled vapor balance and buffering capacity in the node can be expressed as:

$$\frac{dM}{dt} = \frac{dw}{d\varphi} \cdot \frac{d\varphi}{dt} \cdot A \cdot d_e \tag{A.28}$$

Basically, the left term is the total flux of moisture to and from the node and the right term is the combination of the change in total volumetric moisture content of a material, *w*, as a function of the relative humidity, φ, multiplied with the change of φ over the specific time, *t*, and finally multiplied with the volume of the moisture buffering material, $A \cdot d_e$.

According to Figure 9:

$$v_{res\_attic} = \frac{\begin{pmatrix} v_e \cdot Kv_{conv}^{leak,\,roof} + v_{in} \cdot (Kv_{conv}^{leak,\,ceil} + Kv^{ceil}) \\ + v_{supply} \cdot Kv_{leak}^{vent,\,sup} + v^{surf\,1} \\ \cdot Kv_{conv}^{sr1,\,roof} + v^{surf\,2} \cdot Kv_{conv}^{sr2,\,roof} \end{pmatrix}}{Kv_{attic}} \tag{A.29}$$

in which

$$Kv_{attic} = \begin{pmatrix} Kv_{conv}^{leak,\,roof} + Kv_{conv}^{leak,\,ceil} + Kv^{ceil} \\ + Kv_{leak}^{vent,\,sup} + Kv_{conv}^{sr1,\,roof} + Kv_{conv}^{sr2,\,roof} \end{pmatrix} \tag{A.30}$$

From the reduction of conductances in Figure 11, the summarized total conductance Kv_{res_attic} can be defined as:

$$\frac{1}{Kv_{res\_attic}} = \frac{1}{Kv_{attic}} + \frac{z}{A_{surf}} \tag{A.31}$$

$$\frac{1}{kv_{z\_joists}} = \frac{z}{A_{surf\_joists}} = \frac{z_{si} + \dfrac{d_{e\_joists}}{2 \cdot \delta_v}}{A_{surf\_joists}} \tag{A.32}$$

Furthermore, the change in the total volumetric moisture content of the buffering material is obtained:

$$\begin{aligned} &\frac{dw_{joists}}{d\varphi} \cdot \frac{d\varphi}{dt} \cdot A_{surf\_joists} \cdot d_e \\ &= Kv_{res\_attic} \cdot (v_{res\_attic} - v_{joists}) \end{aligned} \tag{A.33}$$

$$\begin{aligned} \frac{dw_{joists}}{dt} &= \frac{Kv_{res\_attic} \cdot (v_{res\_attic} - v_{joists})}{A_{surf\_joists} \cdot d_e} \\ &= \frac{w_{joists,\,j+1} - w_{joists,\,j}}{t_{j+1} - t_j} \end{aligned} \tag{A.34}$$

The total moisture content of the joists, w_{joists}, for the forthcoming time step, $j + 1$, is then expressed as:

$$w_{joists,\,j+1} = \left(w_{joists,\,j} + \frac{Kv_{res\_attic} \cdot (v_{res\_attic} - v_{joists}) \cdot (t_{j+1} - t_j)}{A_{surf\_joists} \cdot d_e} \right) \tag{A.35}$$

Hence, the vapor content of the joists, v_{joists}, for the forthcoming time step, $j + 1$, is

$$v_{joists,\,j+1} = \varphi(w_{joists,\,j+1}) \cdot v_{sat}(T_{attic,\,j+1}) \tag{A.36}$$

Finally, the vapor content of the attic air, v_{attic}, is obtained:

$$v_{attic} = \frac{v_{joists} \cdot Kv_{z\_joists} + v_{res\_attic} \cdot Kv_{attic}}{Kv_{z\_joists} + Kv_{attic}} \tag{A.37}$$

Vapor Content of the Indoor Air, v_{in}

Similar to the attic space, there is an assumed moisture buffering capacity of materials inside the living space. There are two assumed types of materials, wood and gypsum, in accordance with ASHRAE Standard 90.2 (2007), Section 8.8.2.

According to Figure 9, the indoor residual vapor content, v_{res_in} , is defined as:

$$V_{res\_in} = \frac{\begin{pmatrix} v_{attic} \cdot (Kv_{conv}^{leak,\,ceil} + Kv^{ceil}) + v_e \\ \cdot (Kv^{airing} + Kv_{diff}^{wall}) + v_{supply} \\ \cdot Kv^{vent,\,sup} + G_{in} \end{pmatrix}}{Kv_{in}} \tag{A.38}$$

in which

$$Kv_{in} = Kv_{conv}^{leak,\,ceil} + Kv^{ceil} + Kv^{airing} + Kv_{diff}^{wall} + Kv^{vent,\,sup} \tag{A.39}$$

As shown in Figure 12, the residual vapor contents of the two separated networks, $v_{res\_and\_wood}$ and $v_{res\_and\_gyps}$, are defined as:

$$v_{res\_and\_wood} = \frac{v_{res\_in} \cdot Kv_{in} + v_{gyps} \cdot Kv_{z\_in\_gyps}}{Kv_{in} + Kv_{z\_in\_gyps}} \tag{A.40}$$

and

$$v_{res\_and\_gyps} = \frac{v_{res\_in} \cdot Kv_{in} + v_{wood} \cdot Kv_{z\_in\_wood}}{Kv_{in} + Kv_{z\_in\_wood}} \tag{A.41}$$

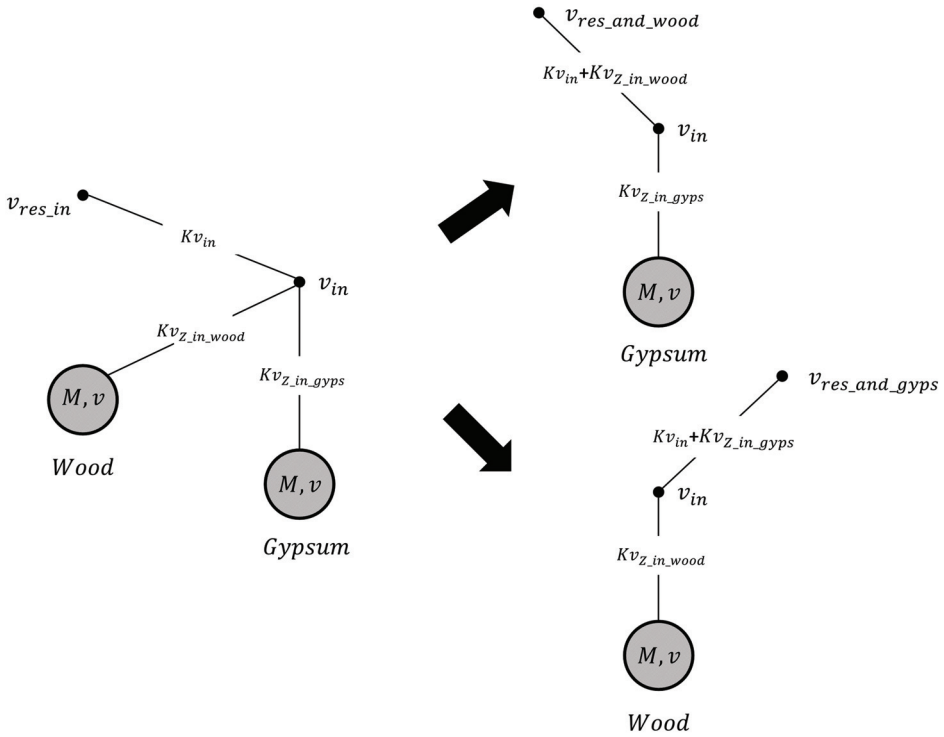

Figure 12 *A network separation of the water vapor transfer balance of the indoor space, where the two moisture buffering materials are extracted into two different networks.* M *is the total moisture weight of the buffering material and* v *is the vapor content.*

The total volumetric moisture content can be defined, for the wooden materials for the next coming simulation step, $j + 1$, as:

$$w_{wood,\,j+1} = w_{wood,\,j} + \frac{\left(\left(\frac{1}{Kv_{z\_wood}} + \frac{1}{Kv_{in} + Kv_{z\_in\_gyps}} \right)^{-1} \cdot (v_{res\_and\_wood} - v_{wood}) \cdot (t_{j+1} - t_j) \right)}{A_{surf\_wood} \cdot d_{e\_wood}} \quad \text{(A.42)}$$

The vapor content of the wood material is then:

$$v_{wood,\,j+1} = \varphi(w_{wood,\,j+1}) \cdot v_{sat}(T_{in,\,j+1}) \quad \text{(A.43)}$$

The same procedure is valid for the assumed moisture buffering materials of gypsum, where the volumetric moisture content for the next coming simulation step, $j + 1$, is:

$$w_{gyps,\,j+1} = w_{gyps,\,j} + \frac{\left(\left(\frac{1}{Kv_{z\_gyps}} + \frac{1}{Kv_{in} + Kv_{z\_in\_wood}} \right)^{-1} \cdot (v_{res\_and\_wood} - v_{gyps}) \cdot (t_{j+1} - t_j) \right)}{A_{surf\_gyps} \cdot d_{e\_gyps}} \quad \text{(A.44)}$$

and

$$v_{gyps,\,j+1} = \varphi(w_{gyps,\,j+1}) \cdot v_{sat}(T_{in,\,j+1}) \quad \text{(A.45)}$$

Finally, as shown in Figure 12, the vapor content of the indoor air is:

$$v_{in} = \frac{\left(v_{res\_in} \cdot Kv_{in} + v_{in\_wood} \cdot Kv_{z\_in\_wood} + v_{in\_gyps} \cdot Kv_{z\_in\_gyps} \right)}{Kv_{in} + Kv_{z\_in\_wood} + Kv_{z\_in\_gyps}} \quad \text{(A.46)}$$

REFERENCES

ASHRAE. 2005. *ASHRAE Handbook—Fundamentals*, Chapter 29, Residential Cooling and Heating Load Calculation. Atlanta: ASHRAE.

ASHRAE. 2007. ANSI/ASHRAE Standard 90.2-2007, *Energy-Efficient Design of Low-Rise Residential Buildings*. Atlanta: ASHRAE.

ASHRAE. 2011. Addendum a to ANSI/ASHRAE Standard 160-2009, *Criteria for Moisture-Control Design Analysis in Buildings*. Atlanta: ASHRAE.

ASHRAE. 2012. Addendum n to ANSI/ASHRAE Standard 62.2-2010, *Ventilation and Acceptable Indoor Air Quality in Low-Rise Residential Buildings*. Atlanta: ASHRAE.

Christian, J.E., and H. Trechsel. 1994. *Moisture control in buildings*. Philadelphia: ASTM.

DIN. 2012. DIN 68800-2 (2012-02), *Wood Preservation – Part 2: Preventive Constructional Measures in Buildings*. Berlin: Deutsches Institut für Normung.

Hagentoft, C.-E., A. Sasic Kalagasidis, M. Thorin, and S.F. Nilson. 2008. Mould growth control in cold attics through adaptive ventilation. Presented at the 8th Nordic Symposium on Building Physics, Copenhagen.

Hamby, D.M. 1994. A review of techniques for parameter sensitivity analysis of environmental models. *Environmental Monitoring and Assessment* 32(2):135–54. DOI: 10.1007/bf00547132

Hukka, A., and H.A. Viitanen. 1999. A mathematical model of mould growth on wooden material. *Wood Science and Technology* 33.

ICC. 2011. *2012 International Energy Conservation Code—Residential Energy Efficiency.* Country Club Hills, IL, USA: International Code Council, Inc.

Kalamees, T., J. Vinha, and J. Kurnitski. 2006. Indoor humidity loads and moisture production in lightweight timber-frame detached houses. *Journal of Building Physics* 29:219–46.

Künzel, H.M. 1995. Simultaneous Heat and Moisture Transport in Building Components. One- and two-dimensional calculation using simple parameters. Dissertation, University Stuttgart, IRB Verlag. Retrieved from www.WUFI.com

Lstiburek, J. 2006. Understanding attic ventilation. *ASHRAE Journal* 48(4):36–45.

MathWorks. 2013. MATLAB®. The MathWorks, Inc., Natick, MA.

Ojanen, T., R. Peuhkuri, H.A. Viitanen, K. Lähdesmäki, J. Vinha, and K. Salminen. 2011. Classification of material sensitivity –New approach for mould growth modeling. Presented at the 9th Nordic Symposium on Building Physics, Tampere, Finland.

Pallin, S. 2012. Probabilistic Risk Assessment of Energy Efficient Retrofitting Techniques – Focus on Multi-family Dwellings and the Effects of Changing Air Movements. Licentiate, Chalmers University, Gothenburg, Sweden.

Polly, M., M. Gestwick, M. Bianchi, R. Anderson, S. Horowitz, C. Christensen, and R. Judkoff. 2011. A method for determining optimal residential energy efficiency retrofit packages. For Building America—Building Technologies Program by National Renewable Energy Laboratory, Golden, CO, USA.

Rudd, A. 2005. Field performance of unvented cathedralized (UC) attics in the USA. *Journal of Building Physics* 29(2):145–69. DOI: 10.1177/1744259105057695

Russell, M., M. Sherman, and A. Rudd. 2007. Review of residential ventilation technologies. *HVAC&R Research* 13(2):325–48. DOI: 10.1080/10789669.2007.10390957

Straube, J., J. Smegel, and J. Smith. 2010. Moisture-safe unvented wood roof systems. Buildingscience.com.

Vose, D. 2008. *Risk Analysis: A Quantitative Guide*, 3rd ed. Hoboken, NJ: Wiley.

Yik, F.W.H., P.S.K. Sat, and J.L. Niu. 2004. Moisture generation through Chinese household activities. *Indoor and Built Environment* 13:115–31.